Article

A Mathematical Model of Glomerular Fibrosis in Diabetic Kidney Disease to Predict Therapeutic Efficacy

Haryana Y. Thomas[1] and Ashlee N. Ford Versypt[1,*]

[1]Department of Chemical and Biological Engineering, University at Buffalo, The State University of New York, Buffalo, NY, USA
[*]Correspondence: ashleefv@buffalo.edu

ABSTRACT Diabetic kidney disease (DKD) is a growing health problem that affects a significant portion of the global population. With a rising global patient number of over 135 million and a yearly incident case of over 2 million, the burden of DKD is rising. Glomerular fibrosis is tissue damage that occurs within the kidney of DKD patients for which effective therapeutic treatments are lacking. One of the reasons for the lack of therapeutic efficacy is glycemic memory where even after blood glucose within diabetic patients is regulated, glomerular fibrosis due to the initial high blood glucose continues to progress. This phenomenon is readily observed in diabetic patients who receive pancreatic transplant for blood glucose regulation where the glomerular fibrosis takes 10 years for full recovery to be observed. In pursuit of determining why it takes a long time for glomerular fibrosis to be reversed, we developed a mechanistic systems biology model of glomerular fibrosis in diabetes from a previous model of interstitial fibrosis. The adapted model consists of a system of ordinary differential equations that models the complex disease etiology and progression of glomerular fibrosis in diabetes. Within the scope of the mechanism we incorporated, we found that advanced glycation end products, which are matrix proteins that are modified due to high blood glucose, are the reason for the delay in the recovery of glomerular fibrosis. The idea that advanced glycation end products are one of the key mediators of glycemic memory is well known in the broad scope of diabetes and its many complications. The mechanism for how advanced glycation end products cause a delay in the recovery of glomerular fibrosis, however, is less established. Following that, the mechanism for why therapeutics targeting glycemic memory such as aminoguanidine, and alagebrium lack efficacy is also not well established. Using our model, we postulate that glucose control, and aminoguanidine are not effective because they do not remove accumulated advanced glycation end products. Further, our model predicts that treatments breaking down advanced glycation end products, such as alagebrium, would be the most efficacious at reversing glomerular fibrosis. Our model helps explain the lack of efficacy of alagebrium at treating advanced glomerular fibrosis due to the inability of alagebrium to reduce TGF-β. There is a well-known therapeutic treatment efficacy reduction when treatment is applied to advanced glomerular fibrosis compared to early glomerular fibrosis. We postulate that two different mechanisms associated with short lived advanced glycation end products and long-lived advanced glycation end products can explain the difference in the response to treatment of glomerular fibrosis when treatment is applied to early glomerular fibrosis vs advanced glomerular fibrosis. Using our systems biology model, we illuminate mechanistic understanding of disease etiology of glomerular fibrosis in diabetes, and then we provide mechanistic explanations for the lack of efficacy of different pharmacological agents at treating glomerular fibrosis. This understanding can enable the development of therapeutics that are more efficacious at treating kidney damage in diabetes.

1 INTRODUCTION

Diabetic kidney disease (DKD) is a significant global health problem. With a rising global patient number of over 135 million, and a yearly incident case of over 2 million, the burden of DKD is rising (1). The death toll of around 0.5 million deaths per year make DKD the second leading cause of mortality among chronic kidney disease patients (1). DKD is a chronic disease for which therapeutic treatments that can prevent, and completely reverse kidney damage are lacking. The lack of such efficacious therapeutic treatments combined with the long-lasting nature of DKD results in an ever-increasing global health burden.

DKD is a complex disease that has multiple factors that cause the development and progression of kidney damage. Although hyperglycemia is the initial stimulus for the development of kidney damage in diabetes, its continued progression is mediated by a host of other stimuli such as hypertension, Angiotensin, AGEs, and enhanced oxidative stress (2). These stimuli work both

dependently and independently, both through mechanical and chemical signaling to induce damage such as kidney fibrosis, proteinuria, GFR decline, which all result in kidney failure. Consequently, therapeutic treatments need to be comprehensive to be able to target the multifaceted nature of DKD. Treatment for DKD consists of approaches to reduce the risk of the development and progression of kidney damage depending on the stage of DKD that you are on. If diagnosed very early lifestyle changes such as nutrition, exercise, glycemic, blood pressure and lipid control have the potential to reduce the risk of the progression of DKD (3). As DKD progresses, RAAS and SGLT2 inhibitors are the suggested therapeutic treatments (3). RAAS and SGLT2 inhibitors , although are not cures for DKD, if used early, can significantly reduce the risk of the development and progression of DKD. However, once DKD has advanced, their efficacy becomes limited (4).

One of the reasons for this limited efficacy is the concept of glycemic memory. Glycemic memory is the idea that even after blood glucose has been regulated, the kidney damage continues to progress. This phenomenon of glycemic memory is also observed in patients who receive pancreatic transplant for regulation of their blood glucose levels. Although blood glucose normalization is achieved relatively fast, full recovery of kidney damage is only observed 10 years post pancreatic transplant (5). AGEs, enhanced oxidative stress and epigenetic changes have been strongly implicated in independently or interdependently being responsible for glycemic memory (6–9). Epigenetic changes are still in basic research and AGEs and oxidative stress have been hypothesized to form a vicious cycle that is the major contributor to glycemic memory (7).

Therapeutic treatments targeting AGEs have been developed but have not entered the market for as additional therapies for managing DKD. AGE formation inhibitors such as aminoguanidine and Pyridoxamine had mixed results in clinical trials (10–12). alagebrium, an AGE crosslink breaker, although made it to human clinical trials was not completed (**?**).

Questions associated with glycemic memory such as why glucose control takes years for recovery of kidney damage to occur, what approaches can accelerate the recovery of kidney damage and why are therapeutic treatments for AGEs, species implicated in glycemic memory, not efficacious remain unanswered.

To provide mechanistic explanations for these questions and thus shed more light on mechanisms governing glycemic memory, we developed a mechanistic-mathematical model of diabetes-induced kidney damage, specifically a model of diabetes-induced glomerular fibrosis.

To build our model of diabetes-induced glomerular fibrosis, we adapted a previous model of fibrosis (13). We took the core pieces of the previous model and adapted it for the mechanism of disease progression relevant to fibrosis in glomerulus during diabetes. Then we gathered data of glomerular fibrosis in diabetes to reparametrize the modified model so that it is now a model completely representative of glomerular fibrosis in diabetes. This final model was then used to provide mechanistic insight into the reasons for delayed recovery of glomerular fibrosis, approaches to accelerate recovery and for generating mechanistic explanations for the lack of therapeutic efficacy.

2 MECHANISM IDENTIFICATION

In this section, we discuss the process of identification of the mechanism for the progression of glomerular fibrosis during diabetes. For the identification of the mechanism of glomerular fibrosis in diabetes, we took inspiration from previously published model of interstitial fibrosis in lupus. We took the mechanism for the progression of interstitial fibrosis in lupus and tried to identify the mechanistic pieces that were relevant to glomerular fibrosis in diabetes. This was done by comparing the mechanistic details of the interstitial lupus fibrosis model to published in vitro experimental studies, in vivo experimental studies, and also well-established protein enzyme interactions. The determined mechanism for the progression of glomerular fibrosis in diabetes is shown in figure 1.

In the interstitial lupus fibrosis model, the mechanism of fibrosis occurs through the recruitment of macrophages that cause the activation of resident cells, which then produce excess quantities of extracellular matrix resulting in fibrosis. To identify the mechanism of glomerular fibrosis in diabetes, we searched the literature for the mechanisms of the production and degradation of collagen, and the cell types and biomolecules involved in the initiation and progression of high blood glucose induced glomerular fibrosis.

2.1 Collagen degradation

The mechanism of glomerular fibrosis progression in diabetes was built upon well-established protein enzyme interactions. Collagen is a protein molecule which is known to be degraded by the enzyme matrix-metalloproteinase (MMP) and MMP is an enzyme which is known to be inhibited by tissue inhibitor of metalloproteinases (TIMP). These proteins, enzymes and inhibitors are upregulated and downregulated in the in vitro diabetic model (14–16) indicating that their involvement is pertinent to the progression of glomerular fibrosis.

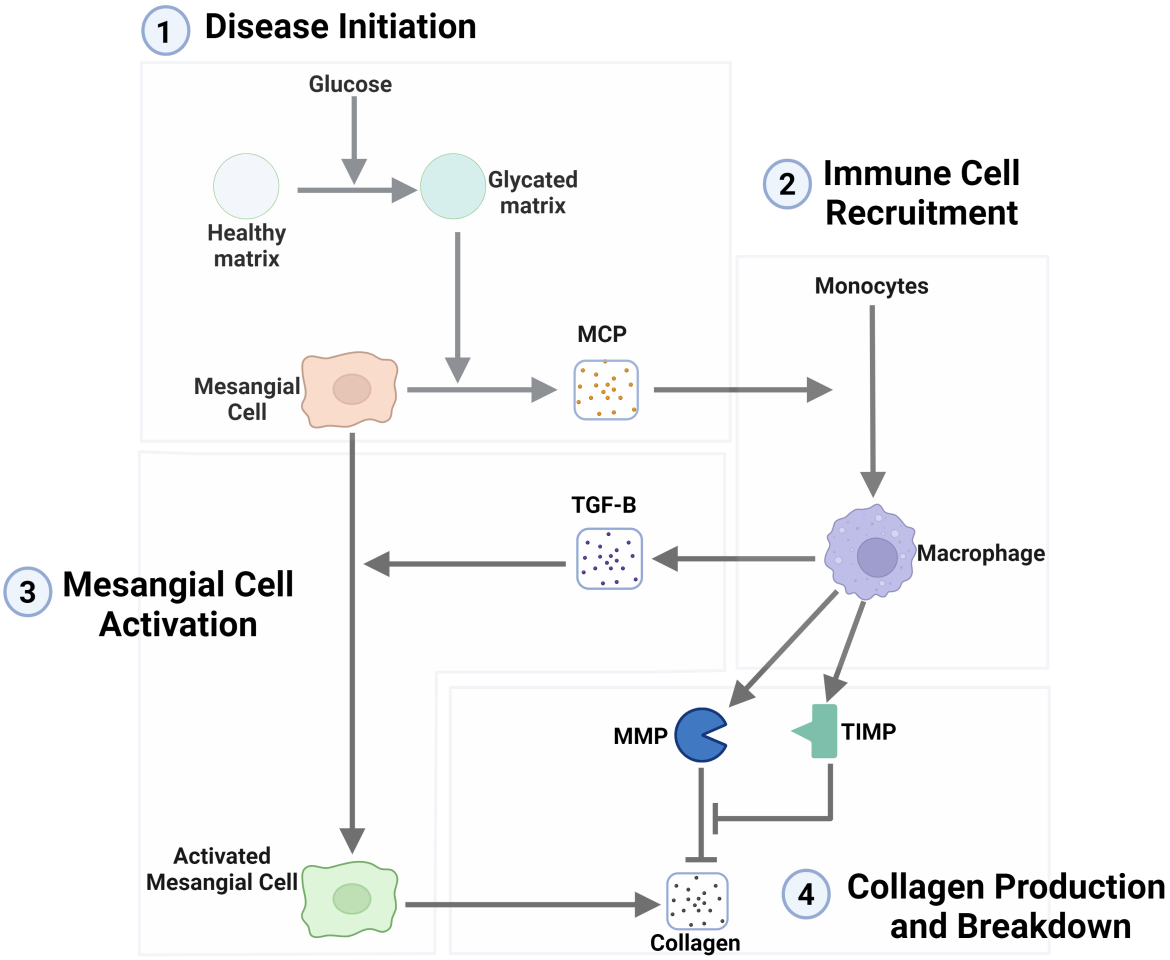

Figure 1: Network representation for the mechanism of the progression of glomerular fibrosis in diabetes. AGE: advanced glycation end products, MCP: monocyte chemoattractant protein, TGF-β: transforming growth factor–β, MMP: matrix metalloproteinase, TIMP: tissue inhibitor of metalloproteinase. Degradation terms are not shown in this figure but are not shown in figures in the parameter estimation section. Macrophages and activated mesangial cells have death rates which are also shown in the figures in the parameter estimation section.

2.2 Excess collagen production

Having identified the mechanism for the degradation of collagen, we then identified the mechanism for the source of collagen. In vitro studies of mesangial cells that are incubated in high glucose, a model representative of the glomerulus in diabetes, showed that collagen protein was significantly upregulated (17–20). This is concurrent with in vivo studies in spontaneously diabetic mice which have significant amounts of collagen deposited in the mesangium of the glomerulus after a couple of weeks of being hyperglycemic (21–29). What isn't clear from these studies is whether it's the quiescent mesangial cell that is producing excess collagen or if it's a different phenotype of the mesangial cell that is producing excess collagen. In other well defined fibrosis mechanisms, it is known that fibroblasts (resident cells) get activated to become myofibroblasts which is a phenotype that is increasingly fibrotic and leads to the excess production of collagen (13). In vitro mesangial cell studies do not explicitly state that activation of the mesangial cell leads to the cell phenotype that is increasingly fibrotic. There have, however, been other studies that have made these parallels of the mesangial cell becoming activated and behaving similarly to the myofibroblast, which is in essence an activated fibroblast. Similarities such as expressing higher amounts of α-smooth muscle actin (α-sma), being more contractile, and producing interstitial collagens, which are all properties exhibited by myofibroblasts (30–32). Mesangial cells can transdifferentiate into myofibroblasts in a process called Myofibroblastic transdifferentiation (MFT) to deposit ECM (33, 34). Thus, we incorporate into our model that it is the activation of mesangial cells that results in the excess

production of collagen.

2.3 Mesangial cell activation

In the interstitial lupus fibrosis model, TGF-β is assigned the role of activating the resident fibroblasts into myofibroblasts. Following the same parallel, we tried to identify whether TGF-β is involved in diabetic glomerular fibrosis in the same capacity as interstitial lupus fibrosis. In vitro studies where mesangial cells are incubated in high glucose (diabetic glomerular fibrosis models) have shown that transforming growth factor beta (TGF-β) is an important mediator of fibrosis as shown by its upregulation in high glucose conditions (19, 35). This is concurrent with the many in vivo studies showing its upregulation in the diabetic mice (21, 25, 27, 28, 36) and also studies where its inhibition led to a decrease in collagen accumulation (37). The role of TGF-β as a key regulator of fibrosis is further supported by the many models of fibrosis in other organs and disease cases that have used TGF-β as the key regulator of fibrosis (13, 38, 39) [Islam2022]. It's highly likely that the observed TGF-β-mediated increase in collagen occurs through TGF-β's activation of the mesangial cell to the more fibrotic phenotype (32–34). In other fibrosis scenarios, TGF-β has been implicated in signaling key cell types such as epithelial cells to transition into a more fibrotic phenotype (40). This evidence suggests that TGF-β is indeed the molecule responsible for the activation of mesangial cells. Consequently, we include TGF-β as a key extracellular signaling molecule that is involved in fibrosis through the activation of the mesangial cell.

2.4 TGF-β production

In the lupus fibrosis model, the source of TGF-β is macrophages. In the literature, it is known that macrophages produced MMP 9 which is an MMP that is capable of cleaving collagen IV within the extracellular matrix. It is also known that the extracellular matrix is full of TGF-β that is released when the extracellular matrix becomes degraded. Instead of incorporating the entire mechanism, we kept it such that macrophages produce TGF-β, which is mechanistically similar to macrophages producing MMP which then causes the release of TGF-β.

The recruitment and accumulation of macrophages within the glomerulus during diabetes is well documented. Many in vivo studies within diabetic mice that show a significant accumulation of macrophages within the glomerulus a short period after the mice develop the diabetic condition (21, 24–27, 29, 41, 42). In vitro coculture studies of mesangial and macrophage cells show that macrophages regulate MMP expression but not TIMP expression while mesangial cells regulate both MMP and TIMP expression (43). This is different from the interstitial lupus fibrosis case where macrophages regulate both MMP, TIMP and the resident fibroblast cell has no role in MMP, and TIMP regulation. Currently in our model, macrophages are the source of MMP and TIMP but in the future changes need to be made to account for the observed mechanistic difference.

2.5 Macrophage recruitment

Macrophages are part of the general human immune response to injury and as such they can be found in different parts of the human body during different disease scenarios where there is cellular damage. Macrophages are known to be recruited to the site of damage via the production of chemoattractant by the damaged cell. This enables the macrophages to pinpoint and arrive to the site of damage by following the chemoattractant up the concentration gradient. So, we assume that macrophages arrive to the glomerulus through the same mechanism of chemoattractant mediated recruitment of macrophages. This is supported by in vitro findings which show that mesangial cells produce monocyte chemoattractant protein (MCP) in the in vitro, diabetic, glomerular-fibrosis model (43). Additionally, MCP is known as a chemoattractant commonly associated with the recruitment of macrophages.

2.6 Disease initiation mechanism

MCP is expressed by mesangial cells when they are cultured with advanced glycation end products (AGEs), which are altered matrix components observed in the diabetic condition (44, 45). The upregulation of MCP is also observed in mesangial cells cultured in high glucose (43) and also in vivo during diabetic induced fibrosis (34), further supporting the mechanism of MCP mediated recruitment of macrophages.

In addition to the effect that AGEs have on mesangial cells, we know that AGEs are significantly accumulated within the mesangial matrix in diabetic conditions (46–48). We also know that AGEs are strongly implicated in the progression of glomerular damage in diabetes especially because when extracellular matrix is incubated in high glucose conditions it leads to the formation of AGEs. As such it fits perfectly within our disease initiation mechanism where high glucose leads to AGE formation which then leads to the stimulation of mesangial cells to produce MCP which leads to the recruitment of macrophages and thus starts the process of fibrosis.

3 MODEL EQUATIONS

In the following section, we describe the equations used to model glomerular fibrosis in diabetes along with the specific biological interpretation of each of the terms in the equations and also how the equations for the model were derived.

A mathematical model for fibrosis in lupus nephritis was built by Hao et al. (13) and our approach has been to adapt the mathematical pieces from their model to model glomerular fibrosis in diabetes. In this adapted mathematical model, there are a total of 10 species that are the key cells and biomolecules involved in the process of glomerular fibrosis in diabetes. The 11 species consist of 3 cell types, namely mesangial cells, activated mesangial cells and macrophages. The remaining 7 species are biomolecules consisting of glucose, AGE, MCP, the growth factor TGF-β, collagen protein and the enzymes involved in its degradation, namely MMP and TIMP (Figure 1).

The population dynamics of each of the species is dependent on specific biologtical processes that lead to changes in their concentration within the glomerulus. The main mechanisms that lead to changes in biomolecule concentration are their production by specific cells within the glomerulus and their natural and enzymatic degradation. The main mechanisms that lead to changes in cellular population are the proliferation of cells, infiltration of immune cells, differentiation of resident cells and also each of the cell's natural death.

Each of these biological processes are modeled using mass action, Michaelis-Menten, and hill function type kinetics. The mass action kinetics states that the rate at which a specific molecule C that is produced by reactants A and B is dependent on the concentrations of A and B and some rate constant k. This approach is mainly used in the production and degradation of biomolecules. For biological processes where cells are activated by a biomolecule to a phenotypic change or where cells are stimulated by a biomolecule to produce another biomolecule, Michaelis Menten or hill function type kinetics is used. We use Michaelis Menten or hill function type kinetics because the stimulation of the cell is through a biomolecule interacting with the receptors on the cell is a receptor limited process. The receptors become saturated and thus even at very large ligand concentration, the rate of cellular stimulation by ligands reaches a maximum. The use of Michaelis Menten or hill function type kinetics for modeling the stimulation and activation of cells is a common approach (13, 49).

Using these modeling approaches and adapted equations from interstitial-lupus fibrosis model, the following set of equations were defined to model each of the steps within the progression of glomerular fibrosis in diabetes.

Disease initiation

As described in the mechanism identification section, the progression of glomerular fibrosis in diabetes is initiated by glucose stimulating the formation of AGEs. The resulting AGE dynamics is modeled by

$$\frac{d(AGE)}{dt} = \lambda_{AGE} Gluc^m - d_{AGE} AGE \tag{1}$$

where the first term on the right-hand side (RHS) of the equation describe the rate of creation of AGEs, which is dependent on the concentration of glucose (Gluc), the AGE formation rate constant λ_{AGE} and the glucose power term, m. The second term on the RHS of the equation describes the rate of removal of AGE, which is dependent on the degradation rate constant d_{AGE} and the concentration of AGE.

Equation 2 describes the dynamics of MCP (P), the chemoattractant protein that is involved in the recruitment of macrophages. Its dynamics is described as

$$\frac{d(P)}{dt} = P_o + \lambda_{\rho mc} \frac{AGE}{K_{AGE} + AGE} mc - d_P P \tag{2}$$

where the first two terms on the RHS of the equation dictate the baseline production of MCP (Po) and the AGE-induced MCP production by mesangial cells (mc). The AGE-induced MCP production by mesangial cells is modeled using Michaelis Menten kinetics where $\lambda_{\rho mc}$ and K_{AGE} represent the production rate and saturation constant for the AGE induced MC production of MCP. The last term in Equation 2 represents the rate of removal of AGEs from the glomerulus.

3.1 Immune cell recruitment

The population dynamics of the macrophages recruited by MCP is modeled as

$$\frac{d(M)}{dt} = \alpha \frac{P^n}{K_P^n + P^n} M_o - d_M M \tag{3}$$

where the first term on the RHS of the equation represents the MCP dependent recruitment of macrophages (M) from the blood. This recruitment is modeled using a hill function where α, K_P and n represent the recruitment rate, saturation constant

and hill function parameter, respectively, for the MCP mediated recruitment of macrophages. The second term on the RHS of the equation represents the removal rate of macrophages from the glomerulus as a result of death or a phenotypical switch.

3.2 Mesangial cell activation

The dynamics for TGF-β (T_B) the growth factor involved in the activation of the mesangial cell is modeled as

$$\frac{d(T_B)}{dt} = T_{Bknot} + \lambda_{T_B M} M - d_{T_B} T_B \tag{4}$$

where the first two terms on the RHS of the equation represent the baseline production of TGF-β and the macrophage mediated production of TGF-β as dictated by the production rate constants T_{Bknot} and λ_{TBM}, respectively. The natural degradation of TGF-β is represented by the last term on the RHS of the equation and dictated by the degradation rate constant d_{T_B}.

The population dynamics for the activated mesangial cell (ma) is modeled as

$$\frac{d(ma)}{dt} = \lambda_{maT} \frac{{T_B}^n}{{K_{T_B}}^n + {T_B}^n} mc - d_{ma} ma \tag{5}$$

where the first term on the RHS of the equation represents the TGF-β mediated activation of mesangial cells and the last term on the RHS of the equation represents the death or apoptosis of activated mesangial cells. The activation of the mesangial cell is modeled through the use of hill function where λ_{maT}, K_{T_B}, and n represent the activation rate constant, saturation rate constant and hill function parameter for the TGF-β mediated activation of the mesangial cell. There is also a removal of the activated mesangial cells from the system through natural death as dictated by the removal rate constant, d_{ma}.

3.3 Collagen production and degradation

Collagen degradation is dependent on the enzymes MMP, TIMP whose kinetics is modeled below. The population dynamics of MMP (Q) is modeled by

$$\frac{d(Q)}{dt} = \lambda_{QM} M - d_{QQr} Q Q_r - d_Q Q \tag{6}$$

where the first, second and third terms represent macrophage mediated production, MMP inhibition by TIMP (Q_r) and natural and enzymatic degradation, respectively (Equation 6) where each term is dictated by its respective rate constant.

Similarly, TIMP dynamics is also modeled by

$$\frac{d(Q_r)}{dt} = \lambda_{Q_r M} M - d_{QrQ} Q_r Q - d_{Qr} Q_r \tag{7}$$

where the first, second and third terms represent macrophage mediated dynamics, TIMP binding with MMP and the natural and enzymatic degradation of TIMP (Equation 7). Each term again being dictated its respective rate constant.

The dynamics of collagen is modeled by

$$\frac{d(\rho)}{dt} = \lambda_{\rho mc} mc + \lambda_{\rho ma} mc - d_{\rho Q} \rho - d_{\rho Q} Q \tag{8}$$

where the first two terms on the RHS of the equation represent the production of collagen by mesangial cells and activated mesangial cells and the last two terms represent the natural degradation of collagen, and the MMP mediated degradation of collagen. Additionally, each of the terms is dictated by a rate constant.

In the determination of the equations for the glomerular fibrosis model, three main criteria were used when adapting equations from the interstitial-lupus fibrosis model. The first is whether the disease progression mechanisms were the same or not. If they were different, then a new set of equations were used to model the newly added biological mechanism. This was done in equations 1 and 2 where the disease initiation mechanism for glomerular fibrosis was different from interstitial fibrosis in lupus. If the mechanisms identified from literature were the same, then the second criteria was used, which was, can the unmodified equations capture the dynamics observed from the gathered experimental data? This was done in equations 3 and 4 where the mechanism identified from literature was the same in both glomerular fibrosis in diabetes and interstitial fibrosis in lupus but the equations did not capture the dynamics observed in the experimental data. As such, the equations were modified to account for the observed experimental dynamics. The third criteria came into play when mechanisms were the same and there was no available experimental data for the dynamics of the species being modeled, as was the case in equation 5,7 and 8. In that case, the model predictions were tested in different scenarios to see if they qualitatively aligned with experimental observations.

4 PARAMETER ESTIMATION

In this section, we discuss the estimation of the model parameters. These model parameters have been calibrated based on a combination of in vivo data, in vitro data, and parameter values obtained from literature (Data gathered is discussed in appendix). Parameters have been estimated using a subsystem approach where only three to four parameters were estimated at once. The estimation was divided such that the parameters involved in the dynamics of one species were estimated and then another species and then the process continued until all parameters were calibrated. As such we discuss the estimation of parameters involving each species separately below.

4.1 Glucose input and AGE dynamics

The glomerular fibrosis model uses an input of blood glucose concentration as stimulus for the progression of fibrosis. For this input, we use the blood glucose concentration of db/db mice over a 20-week period (Figure 2b). This data has been approximated as a ramp input for simplifying the model. This ramp input is fed into the model via the AGE model equation (Equation 1).

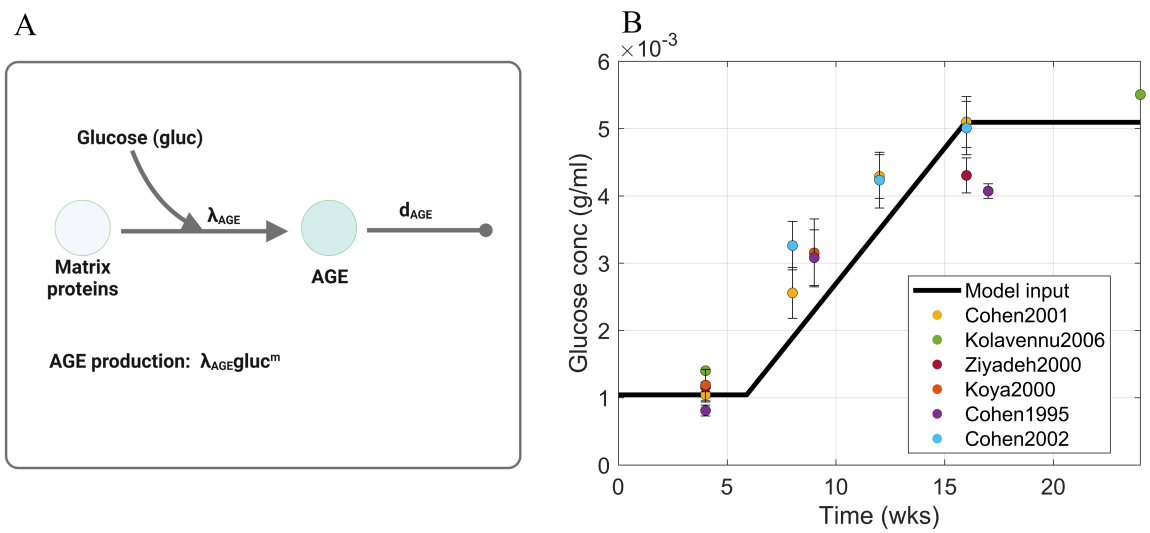

Figure 2: The rate constants and species contributing to the dynamics of AGE (a) blood glucose concentration dynamics within db/db mice approximated as a ramp input (b).

AGEs are formed through the non-enzymatic reaction of glucose with proteins to form a covalently bonded, stable molecule. There are different types of AGEs that can be formed as a result of high glucose concentration within the body such as glycated albumin, hydroimidazolones and glucosepane (50). Out of the many possible AGEs that are formed, Nϵ-(carboxymethyl) lysine (CML) is expressed in the highest quantities in mice (27, 51) relative to other AGEs (27, 52). We assume that it has the highest impact on the progression of fibrosis in diabetes and thus base our AGE dynamics on CML.

In our model, AGE dynamics is dependent on the glucose concentration input (gluc), the rate of formation of AGE (λ_{AGE}), the degradation rate of AGE (d_{AGE}) and the initial value of AGE (AGEss) (Figure 2a). In this case, we overlook the impact of collagen on AGE formation rate.

We calculate the degradation rate of AGE using the half-life of collagen of around 80 days (53). We use the half-life of collagen instead of CML because CML can be enzymatically removed when collagen turnover has occurred which is much faster than the half-life of CML which could be years (50).

The initial value of AGE is assumed to be the carboxymethyl lysine (CML) baseline serum concentration obtained from mice and rat (51, 54). The rate of formation of AGE, obtained by setting the AGE equation (Equation 1) to steady state, is calculated as

$$\lambda_{AGE} = \frac{d_{AGE} AGE_{ss}}{gluc_{ss}^{m}} \tag{9}$$

where $gluc_s s$ is the initial steady state glucose concentration obtained from the glucose input data (Table 1) and m is an

estimated parameter. λ_{AGE} and m are simultaneously calculated by giving m an initial guess, running the model and then comparing AGE concentration fold change to experimental finding that the AGE concentration in the glomerulus of a db/db mice is 20-fold greater at 20 weeks than the initial AGE concentration measured at 7 weeks (47). In this way, we estimate all the parameters involved in AGE dynamics. Their values are shown in Table 1.

4.2 MCP dynamics

For constraining MCP dynamics, in vitro expression of MCP by AGE stimulated mesangial cells was used (Refer to data gathering section for detail). Specifically, the data was used to calibrate the Michaelis-Menten parameters λ_{Pmc} and K_{AGE}, and the baseline MCP production rate Po within Equation 2 (Figure 3a).

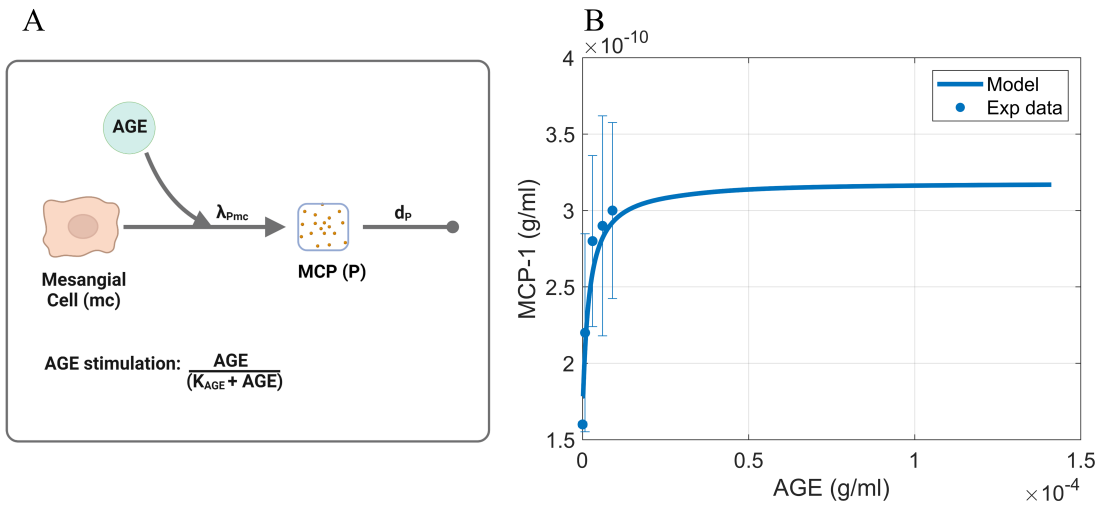

Figure 3: The rate constants and species contributing to the dynamics of MCP (a) Fitting of dose response curve to estimate Michaelis-Menten parameters (b).

The baseline MCP production rate was calculated by setting the MCP equation (Equation 2) to steady state and AGE concentration to zero to obtain

$$P_o = d_P P_{bl} \tag{10}$$

Where d_P is the degradation rate of MCP acquired from literature (13) and P_{bl} is the baseline concentration of MCP in the absence of AGE stimulation, which is obtained from the processed in vitro MCP expression data (Refer to data gathering section for detail).

For estimating the Michaelis-Menten parameters λ_{Pmc} and K_{AGE}, we use the values of P_o and d_P and the in vitro MCP expression data. The acquired values are all shown in Table 1.

4.3 Macrophage dynamics

In our model, the macrophages dynamics is dictated by the macrophage recruitment rate constant, α, the saturation constant for the MCP mediated recruitment of macrophages, K_P, the monocyte concentration in the blood, Mo, and the death/removal rate of macrophages from the glomerulus, d_M (Figure 4a).

To calculate the rate of recruitment of macrophages (α), we set the macrophage equation (Equation 3) to steady state, to obtain

$$\alpha = \frac{d_M M_{ss}}{\frac{P_{ss}^n}{K_P^n + P_{ss}^n} M_o} \tag{11}$$

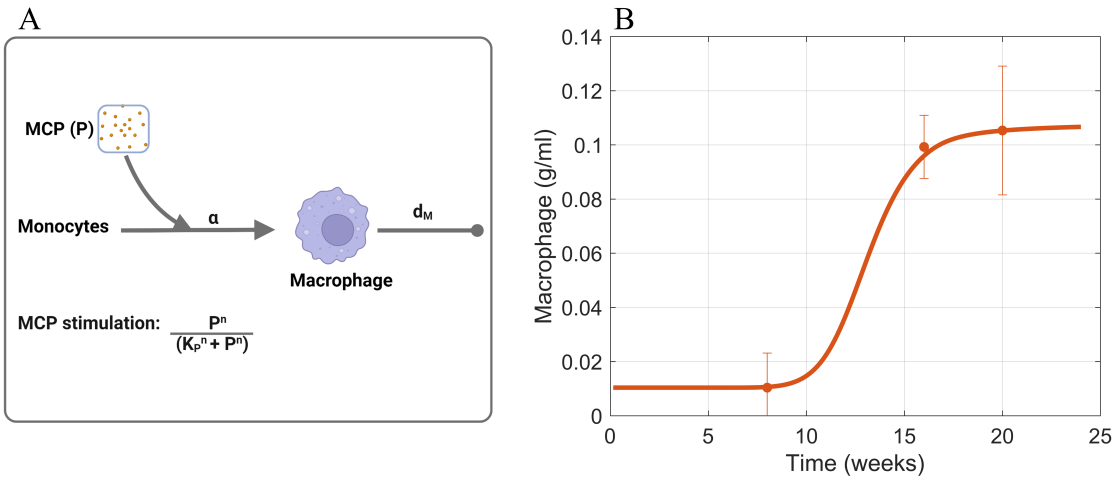

Figure 4: The rate constants and species contributing to the dynamics of macrophages (a) Fitting of macrophage timeseries data to estimate parameters that dictate macrophage dynamics (Equation 3) (b).

Where P_{ss} is the steady state initial value of MCP that causes the initial steady state recruitment of macrophages M_{ss}. P_{ss} is obtained by setting the MCP equation (Equation 2) to zero and solving for the initial steady state value of MCP. The saturation constant K_P is obtained from the literature (13) and n and d_M are parameters that are estimated simultaneously alongside the calculation of α such that the model prediction of macrophage dynamics fits the macrophage timeseries data (Figure 4b). The acquired values are all shown in Table 1.

α, n and d_M are simultaneously estimated such that the model prediction of macrophage dynamics fits the experimental timeseries data of macrophages (Figure 4b).

4.4 TGF-β dynamics

TGF-β dynamics is dictated by the rate of TGF-β production by macrophages, λ_{TB}, the baseline TGF-β production rate, T_{Bknot}, and the degradation rate of TGF-β, d_{TB} (Figure 5a). While d_{TB} is obtained from the literature (13), the baseline and macrophage mediated production rates are estimated using the TGF-β fold change timeseries data (Figure 5b).

4.5 Activated mesangial cell dynamics

Activated mesangial cell dynamics is dependent on a baseline activation of mesangial cells, TGF-β mediated activation, and death/removal of activated mesangial cells from the glomerulus (Figure 6a). To estimate the rate parameters involved in each of those processes, we use a combination of in vitro and in vivo data. The in vitro data is the expression of α-sma by TGF-β stimulated mesangial cells (Refer to data gathering section for detail) and the in vivo data is timeseries α-sma fold change data within the glomerulus.

The in vitro data is used to calibrate the mesangial cell activation rate constant, λ_{maT}, the saturation constant for the TGF-β mediated activation of mesangial cells, and the baseline mesangial cell activation rate, mao (Figure 6a and 6b).

The baseline mesangial cell activation rate constant, mao, was calculated by setting the activated mesangial cell equation (Equation 5) to steady state and setting the TGF-β concentration to zero to obtain

$$ma_o = d_{ma} ma_{ss-vt} \tag{12}$$

Where d_{ma} is the death rate of activated mesangial cells acquired from literature (13) and ma_{ss-vt} is the baseline concentration of activated mesangial cells in the absence of TGF-β stimulation, which is obtained from the processed in vitro α-sma expression data (Refer to data gathering section for detail).

For estimating the Michaelis-Menten parameters λ_{maT} and K_{TB}, we use the values of ma_o and the processed in vitro α-sma

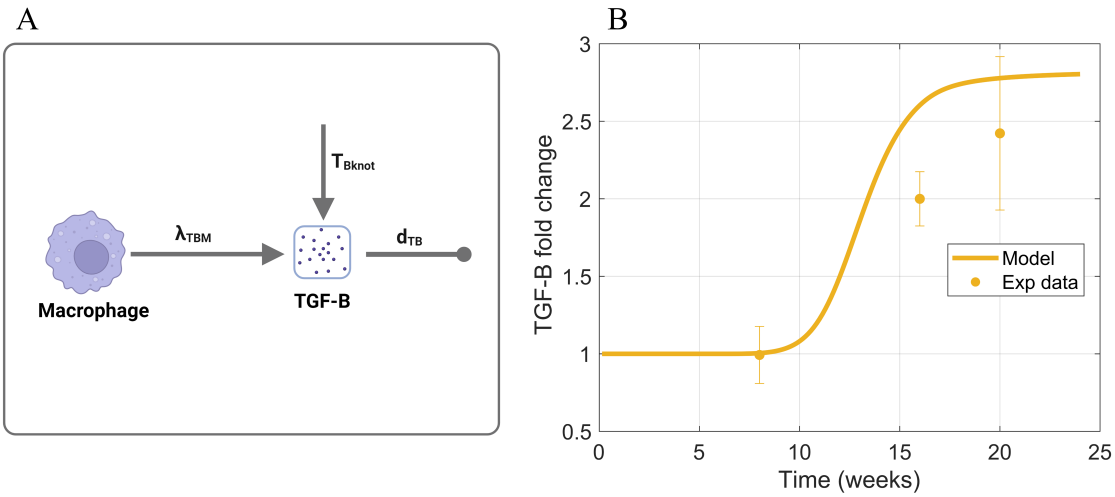

Figure 5: The rate constants and species contributing to the dynamics of TGF-β (a) Fitting of TGF-β timeseries data to estimate parameters that dictate TGF-β dynamics (Equation 4) (b).

expression data. To fit the α-sma data, a new parameter n1 was added to the Michaelis-Menten term. This parameter acts as a compensatory mechanism to account for extra activation of the mesangial cell that is not mediated by TGF-β. This parameter was estimated alongside d_{ma}, a value reestimated to account for additional death/apoptosis of activated mesangial cells in vivo. The acquired values are all shown in Table 1.

4.6 MMP, TIMP and collagen dynamics

MMP and TIMP dynamics is dependent on their production rate constants (λ_{QM} and λ_{QrM}), degradation rate constants (d_Q and d_{Qr}) and binding rate constants ((λ_{QQr} and λ_{QrQ}) (Figure 7a). Parameter values λ_{QM} and λ_{QrM} were modified such that the fold change in expression in diabetic conditions was the same for both such that one does not dominate the other. Due to lack of data for MMP and TIMP within glomeruli during diabetic conditions, no further modifications were made.

Collagen dynamics is dependent on production rate constants ($\lambda_{\rho ma}$ and $\lambda_{\rho mc}$), and degradation rate constants ($\lambda_{\rho Q}$ and λ_{ρ}) (Figure 7a). To constrain the collagen dynamics to experimental data of collagen protein expression fold change, we modified the parameter values for the rate of collagen production by activated mesangial cells ($\lambda_{\rho ma}$) and the MMP mediated degradation rate ($d_{\rho Q}$) (Figure 7b). The acquired values are all shown in Table 1.

4.7 Determination of Initial values

The initial values for each of the species within the model were either obtained from the experimental data found in the literature (AGE and macrophage initial values) or were estimated by setting model equations to zero (Rest of model species). The initial value for AGE within the glomerulus was taken to be the same as the average serum concentration of CML within healthy mice and rats. The initial value of macrophages (Mss) was determined from experimental data where the number of macrophages that were present in the glomerulus before the start of fibrosis had been collected [Figure 4]. This data was then converted into density of macrophages within the glomerulus (g/ml) and used as initial value for macrophages. The acquired values are all shown in Table 1.

The initial values for the rest of the species, namely MCP, TGF-β, activated mesangial cell, MMP, TIMP and collagen were all estimated by setting the model equations to zero and solving for the steady state values of the corresponding species. The estimated values are all shown in Table 2.

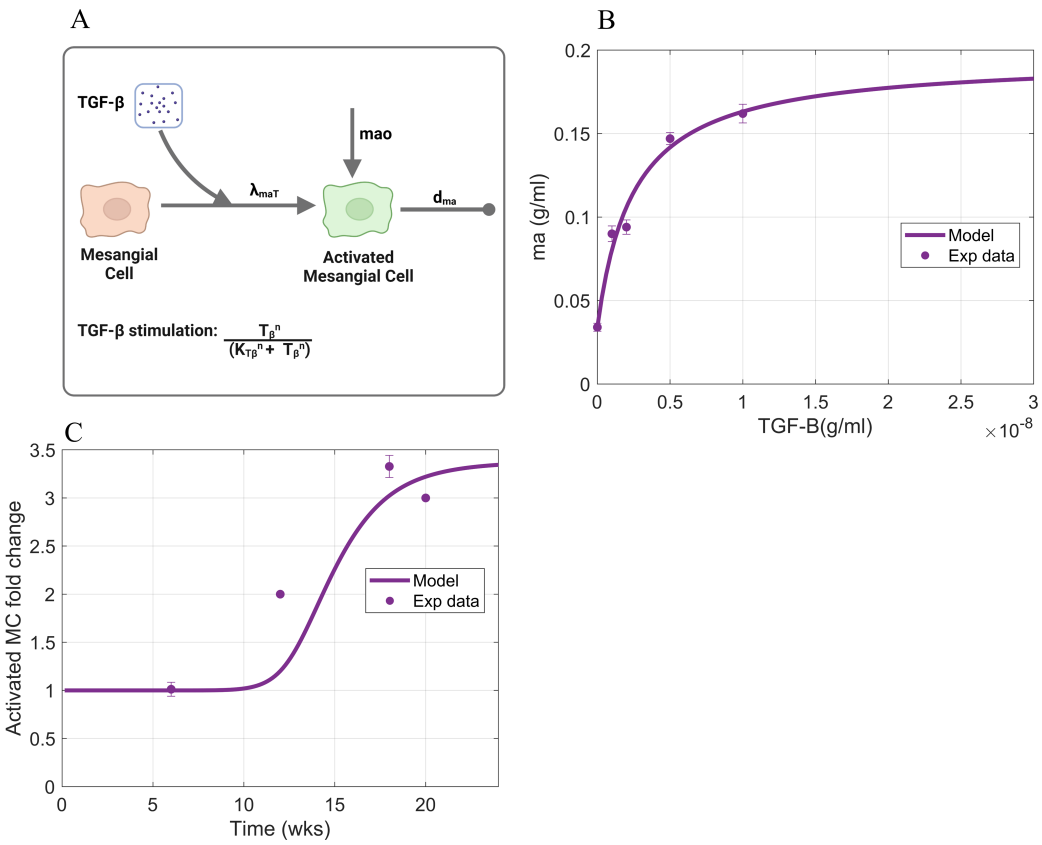

Figure 6: The rate constants and species contributing to the dynamics of activated mesangial cells (a) Fitting of TGF-β induced mesangial cell activation (b) and activated mesangial cell timeseries data (c) to estimate parameters that dictate activated mesangial cells dynamics (Equation 5).

5 RESULTS

It takes over 10 years for glomerular fibrotic tissues to go back to healthy glomerular tissues after pancreatic transplant has been done on patients with glomerular fibrosis (5). Pancreatic transplant allows one to have good blood glucose regulation and thus removes the main stimulus of kidney damage during diabetes (We define good blood glucose regulation as regulation that fixes the blood glucose concentration to baseline levels without the blood glucose levels fluctuating or moving outside of the baseline level). The question that we're interested in answering is why it takes a long period of time for glomerular fibrosis to be reversed after the main stimulus, high blood glucose, has been removed through good blood glucose regulation.

To approach this question, we utilized the adapted mathematical model to gain insight into the mechanistic pieces that prevent glomerular tissues from recovering fast once good blood glucose control had been achieved. Thereafter, our aim was to be able to propose interventions capable of reversing glomerular fibrosis at a faster rate.

The dynamics of the adapted model containing the key cells and biomolecules involved in glomerular fibrosis during diabetes is shown in Figure 8. We see that the blood glucose stimulus, which starts to increase at six weeks and plateau at 16 weeks (Figure 8A) causes an increasing accumulation of AGEs (Figure 8B), which starts the cascade of immune cell recruitment followed by mesangial cell activation and then finally collagen accumulation. Each of the species modeled in this process of glomerular fibrosis reach a steady state within the 24-week time period except for AGEs. The concentration of AGEs does not reach steady state within the given time frame because its degradation rate is very small relative to its formation rate. These model dynamics are the cellular and biomolecular dynamics that is predicted to be occurring within the glomerulus of a db/db mice over a 24-week period.

Our base-case scenario is the scenario which has been locally constrained for the prescribed blood glucose concentration, specific initial condition of cellular and biomolecular species and experimental data of species dynamics. As such, this base-case scenario gives us the blood glucose to glomerular fibrosis relationship that is shown in Figure 8 dynamics. For the given conditions, these results show that a switch in blood glucose concentration from baseline levels (0 to 6 weeks) to high blood

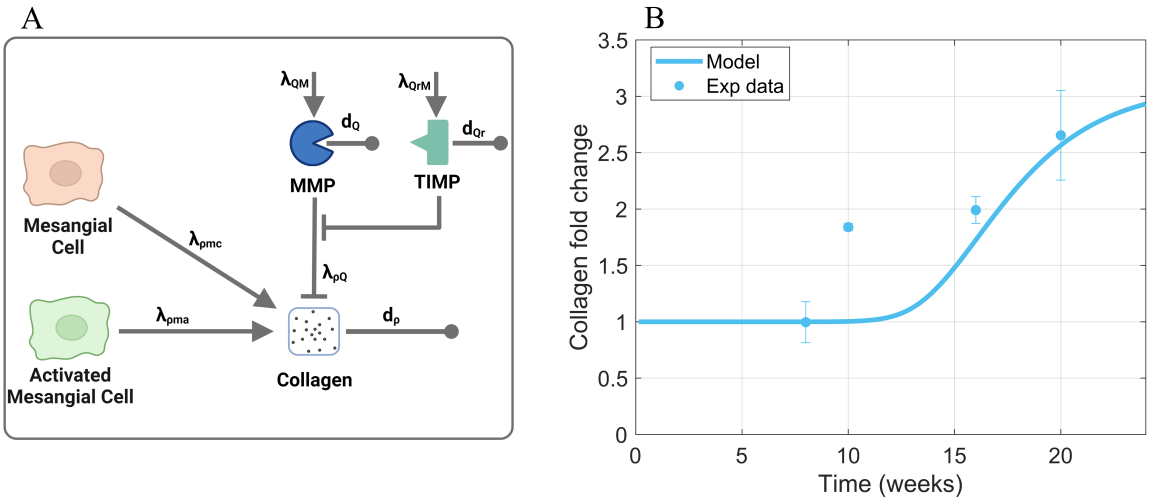

Figure 7: The rate constants and species contributing to the dynamics of MMP, TIMP and collagen (a) Fitting of collagen timeseries data to estimate parameters that dictate collagen dynamics (b).

glucose concentration levels (16 to 24 weeks) results in a similar switch from healthy glomerular tissue (0 to 12 weeks) to a fibrotic glomerular tissue (24 weeks and up) (Figure 8A and 8I).

Now that we have the cellular and biomolecular dynamics of glomerular fibrosis in the diabetic mice, we can run different scenarios to try to see if our model can answer the question of what mechanistic pieces are responsible for the delayed recovery of glomerular fibrosis after good blood glucose control has been achieved. As such, the first simulation that we try is to apply good blood glucose control to our model (Figure 9).

5.1 Efficacy of Glucose Control

Figure 9 shows the results of applying good blood glucose control on glomerular fibrosis. We apply good blood glucose control at 16 weeks and this is observed in Figure 9a by the immediate decrease of blood glucose levels from the elevated state back down to the normal baseline levels and maintained at that baseline level. The resulting effect of good blood glucose control on collagen is that there is no effect observed within the 24 week time period, defined henceforth as the short term period(Figure 9b). We see the profile of collagen is the same as that of the base case scenario and that for an immediate blood glucose regulation, we do not get the same immediate decrease in glomerular fibrosis. To see whether blood glucose control has any effect on glomerular fibrosis in the long run or not, we simulate the model for a longer time period of 200 weeks (approx. 4 years) and we see from the results that there is approximately 5 percent reduction in the extent of glomerular fibrosis (Figure 9d).

Our model predicted that immediate regulation of blood glucose control does not lead to immediate amelioration of glomerular fibrosis. This is in agreement with the experimental observation that blood glucose regulation does not lead to immediate reversal of glomerular fibrosis (5) but that it takes many years for complete reversal to occur.

The next obvious question to ask was, what is the cause of this delayed recovery of glomerular fibrosis? We looked into our model and found that it was the continuously elevated concentration of AGEs that was the cause of the delayed recovery of fibrosis. In Figure 10, in addition to the dynamics of glucose and collagen, we see the species dynamics for AGE and macrophages for the glucose control scenario. What we see in these results is that although glucose concentration is immediately brought down to healthy-baseline levels (Figure 10a), the AGE concentration, which is immediately downstream of glucose in the progression of fibrosis, does not decrease to healthy baseline levels immediately. Rather, we see a slow decline in the concentration of AGEs within the glomerulus, which for the most part is significantly elevated (Figure 10b). This continued significantly elevated levels of AGE causes a persistent stimulation of mesangial cells which results in the persistent recruitment and accumulation of macrophages (Figure 10c). And the continued accumulation of macrophages results in persistent glomerular fibrosis through the continued activation of mesangial cells, the source of the excess collagen (Figure 10d).

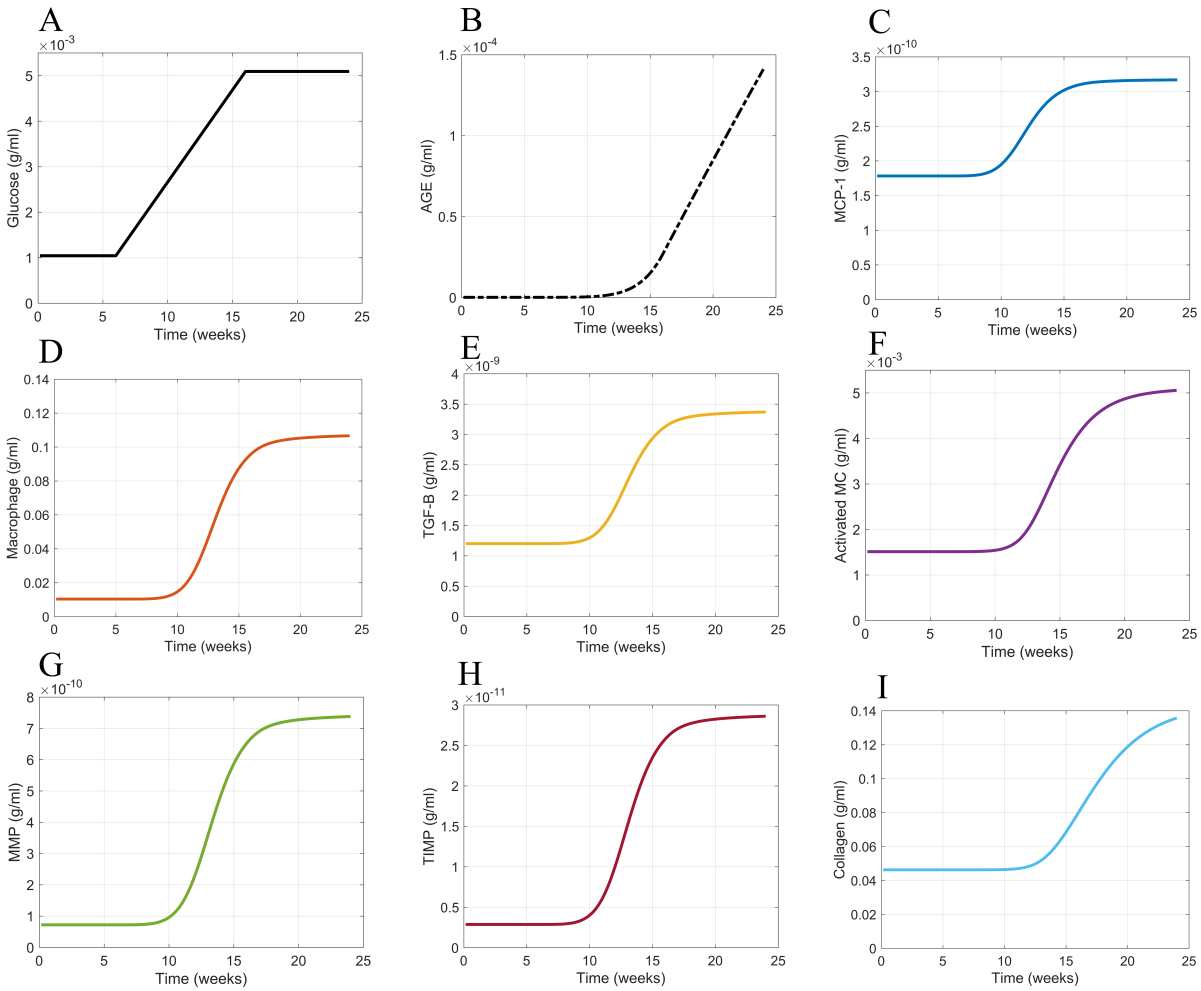

Figure 8: Model simulation dynamics of cells and biomolecules involved in glomerular fibrosis over a period of 24 weeks.

5.2 Efficacy of AGE Inhibition

Having determined that the continuously elevated concentration of AGEs was the cause of the delay in the recovery of glomerular fibrosis, the solution to preventing this delay then is to avert this continued elevated levels of AGE. The first approach that we proposed was to inhibit the production of AGEs to prevent the continuously elevated concentration of AGE (Figure 11a). Concurrent to the other scenarios, the inhibition of AGEs was applied at 16 weeks. What we observe is that the inhibition of AGEs has no impact on glomerular fibrosis, both in the short run and the long run (Figure 11c and 11e). Further, we observe that the dynamics of AGEs in this scenario mirros the dynamics of AGEs in the glucose control scenario (Figure 11d vs 11b) indicaing that the inhibition of AGEs has the equivalent effect of applying glucose control but that it does not have a greater impact than that. As such, its efficacy is limited and does not accelerate the recovery of glomerular fibrosis.

The reason why the inhibition of AGE is ineffective is because treatment was applied at 16 weeks. By this point glomerular fibrosis has developed and AGEs are also significantly accumulated. Inhibition of AGEs only prevents the further production of AGEs and does not remove the already accumulated levels of AGE. It is the already-accumulated levels of AGE that is delaying the recovery of glomerular fibrosis. Consequently, the best approach to accelerate the recovery of fibrosis would be to actively remove the already accumulated AGEs from the system.

5.3 Efficacy of Enhanced AGE Degradation

To test the hypothesis that active removal of AGE will accelerate the recovery of fibrosis, we simulated the model with enhanced removal of AGEs from the system (Figure 12a). We apply a treatment at 16 weeks, which represents the enhanced degradation of AGEs. We observe from the results our hypothesis is correct. We see that in the short run, the enhanced degradation of AGEs

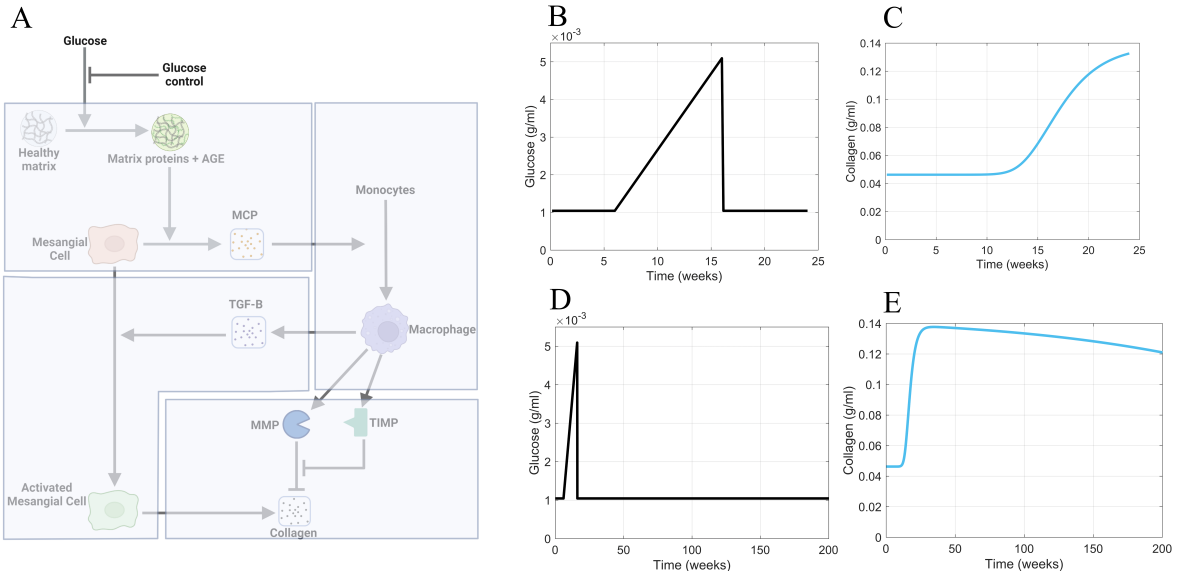

Figure 9: Efficacy of good blood glucose control on reducing glomerular fibrosis in the short term (B,C) and long term (D,E). Network figure to indicate visually blood glucose control (A).

results in the accelerated recovery of fibrosis (figure 12c) and the reason for the immediate recovery is the immediate return of AGE concentration down to healthy baseline levels (Figure 12b).

In conclusion, we developed a model of glomerular fibrosis in diabetes to try to determine the lack of therapeutic efficacy and also to propose more efficacious therapeutic approaches. Our model recapitulates the experimentally observed phenomenon that good blood glucose control does not lead to immediate recovery of glomerular fibrosis in diabetes. We are able to determine using our model that good glucose control is not immediately efficacious due to the accumulation of AGEs and their slow removal from the system. We further propose a more efficacious treatment approach which is that the active removal of AGEs from the glomerulus will result in the accelerated recovery of glomerular fibrosis.

6 DISCUSSION

We consider in our model different therapeutic treatments for advanced glomerular fibrosis. Specifically, we ask the question of why it takes a long time for advanced glomerular fibrosis to be reversed when glucose treatment is applied.

Firstly, our model is able to capture this delayed recovery of advanced glomerular fibrosis when glucose control is applied (Figure 9E). This behavior is observed in patients with advanced glomerular fibrosis whereby glucose control via pancreatic transplant does not result in the immediate recovery of fibrosis but rather takes a very long time (10 years) (5). This complete reversal of advanced glomerular fibrosis has not been shown in animal models because the length of study was not long enough (55). The length of study for normoglycemia post advanced glomerular fibrosis in these rat studies was a maximum of 4 months in which period no reversal of glomerular fibrosis was observed. Non advanced glomerular fibrosis, however, has been shown to be at least partially reversible (56–59).

Our model predicts that it would take around 10 years for complete reversal of glomerular fibrosis to be observed (Figure suppl 1A). Although, we can't compare this value to time it takes for full reversal of advanced glomerular fibrosis in rats, we see that the value is concurrent with the time it takes for advanced glomerular fibrosis to be reversed in humans (5).

Our mechanistic explanation for why reversal of advanced fibrosis takes a long time is that the slow degradation of AGEs results in the persistent stimulation of mesangial cells which leads to the continued recruitment of macrophages which mediate the continued accumulation of collagen through the persistent activation of mesangial cells (Figure 10). The slow degradation of AGEs such as CML is well known. In diabetic rats that have been given pancreatic transplant to achieve normoglycemia after having had diabetes for a period of time show that the collagen glycated AGE content does not decrease even after 4 months of normoglycemia whether it's in the early stage or advanced stage of glomerular fibrosis (55). Our model actually predicts a faster degradation of AGEs (an 11 percent reduction in AGEs four months post normoglycemia) than observed in these rats but even then we see that the reversal of glomerular fibrosis takes a long time. Our model prediction of the persistent accumulation of intermediary species such as MCP, macrophages, TGF-β and activated mesangial cells even after normoglycemia achieved in

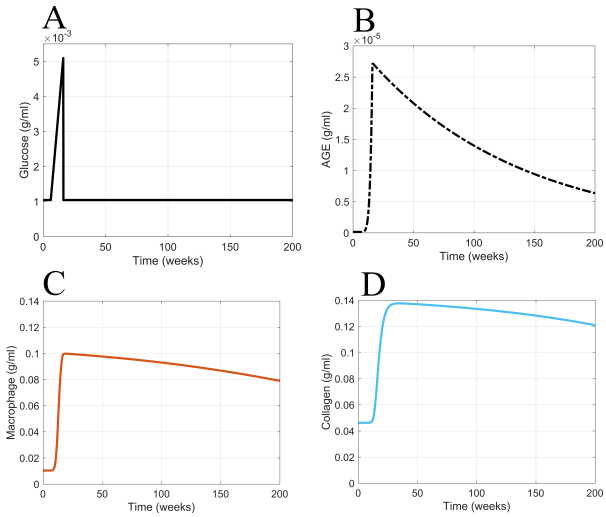

Figure 10: The persistence of AGEs within the glomerulus is the cause for the delayed recovery of fibrosis. Impact of good blood glucose control (A) on AGE concentration (B), Macrophage concentration (C) and collagen concentration (D) in the long run.

diabetic rats has not been studied experimentally and is still an avenue to be explored.

Having found that the slow degradation of AGE is the cause for the delay in the reversal of fibrosis, we had attempted to accelerate the process by inhibiting AGE formation. We found that inhibition of AGE formation did little to accelerate the recovery of fibrosis, and that was because long lived AGEs were already accumulated in the glomerulus. aminoguanidine is a molecule that inhibits the formation of AGEs and has been studied as a potential therapeutic for treating glomerular fibrosis. Although, the efficacy of aminoguanidine on advanced glomerular fibrosis has not been studied, its effect on the development of glomerular fibrosis in diabetic rats has been studied (60). The study found that aminoguanidine reduces TGF-β gene expression within the glomeruli and AGE and Collagen protein expression within the kidney cortex (60). Without the full inhibition of AGE formation, our model is also able to replicate the experimentally observed results of a reduced TGF-β expression and reduced glomerular fibrosis.

Our model predicts that the time it takes for the full recovery of fibrosis with AGE formation inhibition is also 10 years which means that in a short time frame not much recovery will be observed. Clinical trials for AGE formation inhibitors such as aminoguanidine have had limited success (10–12) and one reason could be due to the fact that once glomerular fibrosis has developed, inhibiting AGE formation is not an effective strategy to reverse glomerular fibrosis quickly. Since these clinical trials don't run for long periods of time, the efficacy observed will be small and not statistically significant.

An approach that we determined will be most efficacious at reversing advanced glomerular fibrosis quickly is the active removal of these long live AGEs from the glomerulus. alagebrium, an AGE crosslink breaker capable of breaking down long lived AGEs, such as CML, has been studied as a potential therapeutic target for treating glomerular fibrosis. A study on diabetic rats showed that the early treatment of these rats (16 weeks into diabetes) with alagebrium for 16 weeks was able to reverse glomerular fibrosis almost to normal levels and also reduce the long-lived AGE CML, TGF-β and collagen IV within the renal cortex (61). However, the late treatment of these diabetic rats (24 weeks into diabetes) with alagebrium for 8 weeks, although it was able to reduce CML levels to baseline, was not able to reduce glomerular fibrosis by a statistically significant amount nor was it able reduce TGF-β and collagen IV within the renal cortex by a statistically significant amount (61). This finding seems to be in disagreement with our prediction which states that the enhanced breakdown of long-lived AGEs such as CML would lead to the accelerated reversal of advanced glomerular fibrosis (Figure 12). However, our model predicted that the breakdown of AGEs would be followed by a rapid decrease in TGF-β, which the experimental result does not show. The absence of decrease in TGF-β can explain why a reversal of advanced glomerular fibrosis was not observed because TGF-β, which we know to be the key profibrotic growth factor that mediates fibrosis, was not reduced. Our model is not able to capture this interesting result that the breakdown of AGEs in vivo results in a continued accumulation of TGF-β rather than the expected reduction. This lack of reduction in TGF-β could be due to either the presence of another long-lived AGE which was not degraded by alagebrium or the breakdown of CML, which is glycated collagen, led to the release of bound TGF-β from the collagen matrix. This elevated TGF-β levels when a diabetic rat is treated with alagebrium has also been observed in other studies (62) and as such may be an important mechanism to be further explored experimentally.

An interesting phenomenon that our model is not able to replicate is the different response to treatment between early and

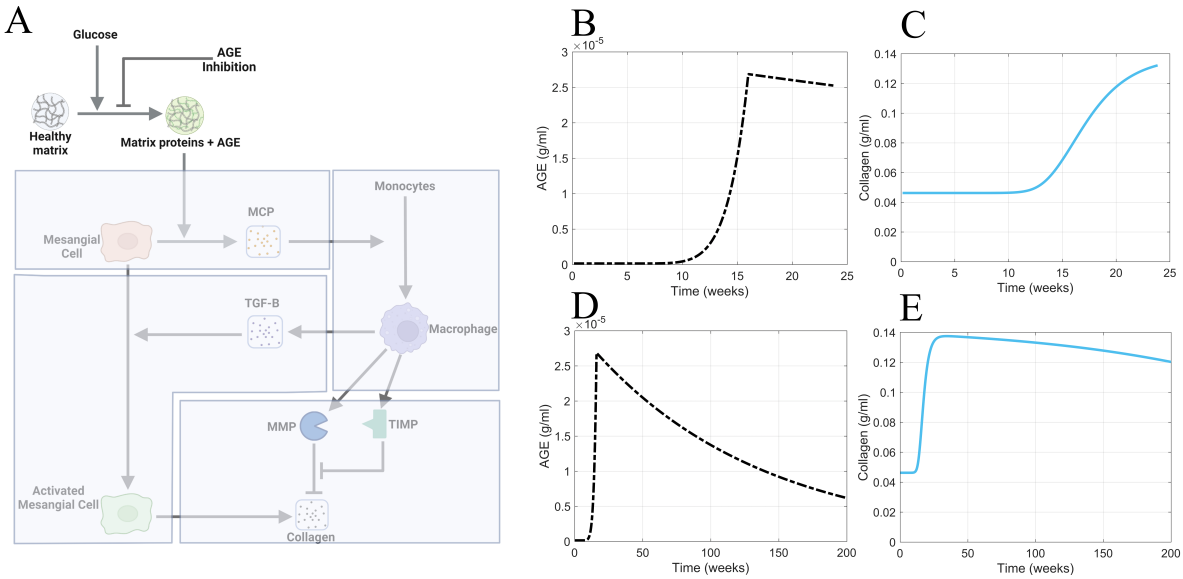

Figure 11: AGE inhibition is not sufficient for accelerating recovery from glomerular fibrosis. Efficacy of AGE inhibiton (B, D) on glomerular fibrosis in the short term (C) and long term (E). Network figure to indicate visually the inhibition of AGE (A).

advanced glomerular fibrosis. Early treatment of glomerular fibrosis, such as 4 months after the development of diabetes, has been shown to be fully reversible within 4 months of normoglycemia (**?**) and late treatment of glomerular fibrosis (8 months post induction of diabetes) has not been shown to be reversible with 4 months of treatment (55). This similar pattern is observed when crosslink breaker alagebrium is used. The investigators observe that an early treatment (4 months post diabetes) is able to reverse the glomerular fibrosis, but late treatment (6 months post diabetes) is not (61). A potential mechanism that can explain this different response in treatment is that the early and late stages of glomerular fibrosis are occurring via different mechanisms. It could be that the early development of glomerular fibrosis is being mediated by short-lived AGEs and the late development of fibrosis is being mediated by long-lived AGEs. Thus, early glomerular fibrosis is reversible because short-lived AGEs are quickly removed from the glomerulus due to their short half-lives whereas late glomerular fibrosis is not quickly reversible due to the long half lives of long-lived AGEs. This is a mechanism we hope to study in future iterations of model.

In conclusion, we developed a model of glomerular fibrosis in diabetes to try to determine the lack of therapeutic efficacy and also to propose more efficacious therapeutic approaches. Our model recapitulates the experimentally observed phenomenon that good blood glucose control does not lead to immediate recovery of glomerular fibrosis in diabetes. We are able to determine using our model that good glucose control is not immediately efficacious due to the accumulation of AGEs and their slow removal from the system. We further propose a more efficacious treatment approach which is that the active removal of AGEs from the glomerulus will result in the accelerated recovery of glomerular fibrosis.

CONFLICT OF INTEREST STATEMENT

The authors declare that the research was conducted in the absence of any commercial or financial relationships that could be construed as a potential conflict of interest.

Acknowledgments

We would like to thank Dr. Stelios T. Andreadis, Dr. Rudiyanto Gunawan, and Dr. Aminul Islam from the University at Buffalo for discussions pertaining to the model and lab members, particularly Eduardo A. Chacin Ruiz and Krutika Patidar, for their thorough feedback on this manuscript.

Funding

This material is based upon work supported by the National Science Foundation under Grant No. 2133411 and resources from the University at Buffalo.

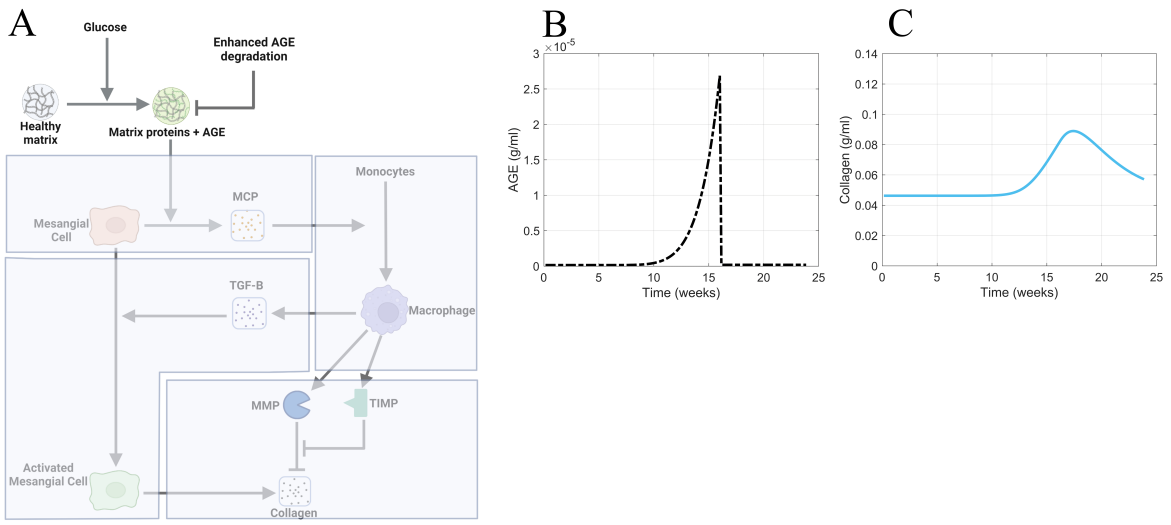

Figure 12: Enhaced AGE degradation is the most efficacious approach for accelerating recovery from glomerular fibrosis. Efficacy of enhanced AGE degradation (B) on glomerular fibrosis (C) in the short term. Network figure to indicate visually the enhanced degradation of AGE (A).

SUPPLEMENTAL DATA

REFERENCES

1. Deng, Y., N. Li, Y. Wu, M. Wang, S. Yang, Y. Zheng, X. Deng, D. Xiang, Y. Zhu, P. Xu, Z. Zhai, D. Zhang, Z. Dai, and J. Gao, 2021. Global, Regional, and National Burden of Diabetes-Related Chronic Kidney Disease From 1990 to 2019. *Frontiers in Endocrinology* 12.

2. Zhang, Q., M. Yang, Y. Xiao, Y. Han, S. Yang, and L. Sun, 2021. Towards better drug repositioning: Targeted immunoinflammatory therapy for diabetic nephropathy. *Current Medicinal Chemistry* 28:1003–1024.

3. Guedes, M., and R. Pecoits-Filho, 2022. Can we cure diabetic kidney disease? Present and future perspectives from a nephrologist's point of view. *Journal of Internal Medicine* 291:165–180.

4. Pillai, A., and D. Fulmali, 2023. A Narrative Review of New Treatment Options for Diabetic Nephropathy. *Cureus* 2:1–7.

5. Fioretto, P., M. W. Steffes, D. E. Sutherland, F. C. Goetz, and M. Mauer, 1998. Reversal of lesions of diabetic nephropathy after pancreas transplantation. *The New England Journal of Medicine* 339:69–75.

6. Yamazaki, T., I. Mimura, T. Tanaka, and M. Nangaku, 2021. Treatment of diabetic kidney disease: current and future. *Diabetes & Metabolism Journal* 45:11–26.

7. Xu, Y., and H. Guo, 2017. Role of Advanced Glycation End Products in the Progression of Diabetes Mellitus. *Global Journal of Obesity, Diabetes and Metabolic Syndrome* 4:024–035.

8. Drzewoski, J., J. Kasznicki, and Z. Trojanowski, 2009. The role of "metabolic memory" in the natural history of diabetes mellitus. *Polskie Archiwum Medycyny Wewnetrznej* 119:493–500.

9. Testa, R., A. R. Bonfigli, F. Prattichizzo, L. La Sala, V. De Nigris, and A. Ceriello, 2017. The "Metabolic Memory" Theory and the Early Treatment of Hyperglycemia in Prevention of Diabetic Complications. *Nutrients* 9.

10. Williams, M. E., W. K. Bolton, R. G. Khalifah, T. P. Degenhardt, R. J. Schotzinger, and J. B. McGill, 2007. Effects of pyridoxamine in combined phase 2 studies of patients with type 1 and type 2 diabetes and overt nephropathy. *American Journal of Nephrology* 27:605–614.

11. Rabbani, N., S. S. Alam, S. Riaz, J. R. Larkin, M. W. Akhtar, T. Shafi, and P. J. Thornalley, 2009. High-dose thiamine therapy for patients with type 2 diabetes and microalbuminuria: A randomised, double-blind placebo-controlled pilot study. *Diabetologia* 52:208–212.

12. Bolton, W. K., D. C. Cattran, M. E. Williams, S. G. Adler, G. B. Appel, K. Cartwright, P. G. Foiles, B. I. Freedman, P. Raskin, R. E. Ratner, F. C. W. Bruce S Spinowitz, and J.-P. Wuerth, 2004. Randomized trial of an inhibitor of formation of advanced glycation end products in diabetic nephropathy. *American Journal of nephrology* 24:32–40.

13. Hao, W., B. Rovin, and A. Friedman, 2014. Mathematical model of renal interstitial fibrosis. *Proceedings of the National Academy of Sciences* 111:14193–14198.

14. Wahab, N. A., and R. M. Mason, 1996. Modulation of neutral protease expression in human mesangial cells by hyperglycaemic culture. *Biochemistry Journal* 320:777–783.

15. McLennan, S. V., S. Y. Martell, and D. K. Yue, 2000. High glucose concentration inhibits the expression of membrane type metalloproteinase by mesangial cells: Possible role in mesangium accumulation. *Diabetologia* 43:642–648.

16. McLennan, S. V., E. J. Fisher, D. K. Yue, and J. R. Turtle, 1994. High glucose concentration causes a decrease in mesangium degradation: A factor in the pathogenesis of diabetic nephropathy. *Diabetes* 43:1041–1045.

17. Ayo, S. H., R. A. Radnik, J. A. Garoni, W. F. Glass, and J. I. Kreisberg, 1990. High glucose causes an increase in extracellular matrix proteins in cultured mesangial cells. *American Journal of Pathology* 136:1339–1348.

18. Ayo, S. H., R. A. Radnik, W. F. Glass, J. A. Garoni, E. R. Rampt, D. R. Appling, and J. I. Kreisberg, 1991. Increased extracellular matrix synthesis and mRNA in mesangial cells grown in high-glucose medium. *American Journal of Physiology - Renal Fluid and Electrolyte Physiology* 260:F185–191.

19. Baccora, M. H., P. Cortes, C. Hassett, D. W. Taube, and J. Yee, 2007. Effects of long-term elevated glucose on collagen formation by mesangial cells. *Kidney International* 72:1216–1225.

20. Haneda, M., R. Kikkawa, N. Horide, M. Togawa, D. Koya, N. Kajiwara, A. Ooshima, and Y. Shigeta, 1991. Glucose enhances type IV collagen production in cultured rat glomerular mesangial cells. *Diabetologia* 34:198–200.

21. Choi, S. R., J. H. Lim, M. Y. Kim, E. N. Kim, Y. Kim, B. S. Choi, Y. S. Kim, H. W. Kim, K. M. Lim, M. J. Kim, and C. W. Park, 2018. Adiponectin receptor agonist AdipoRon decreased ceramide, and lipotoxicity, and ameliorated diabetic nephropathy. *Metabolism: Clinical and Experimental* 85:348–360.

22. Kosugi, T., T. Nakayama, Q. Li, V. A. Chiodo, L. Zhang, M. Campbell-Thompson, M. Grant, B. P. Croker, and T. Nakagawa, 2010. Soluble Flt-1 gene therapy ameliorates albuminuria but accelerates tubulointerstitial injury in diabetic mice. *American Journal of Physiology - Renal Physiology* 298:609–616.

23. Chen, H. Y., X. Zhong, X. R. Huang, X. M. Meng, Y. You, A. C. Chung, and H. Y. Lan, 2014. MicroRNA-29b inhibits diabetic nephropathy in db/db mice. *Molecular Therapy* 22:842–853.

24. Ichinose, K., Y. Maeshima, Y. Yamamoto, M. Kinomura, K. Hirokoshi, H. Kitayama, Y. Takazawa, H. Sugiyama, Y. Yamasaki, N. Agata, and H. Makino, 2006. 2-(8-Hydroxy-6-methoxy-1-oxo-1H-2-benzopyran-3-yl) propionic acid, an inhibitor of angiogenesis, ameliorates renal alterations in obese type 2 diabetic mice. *Diabetes* 55:1232–1242.

25. Hong, Y. A., J. H. Lim, M. Y. Kim, T. W. Kim, Y. Kim, K. S. Yang, H. S. Park, S. R. Choi, S. Chung, H. W. Kim, H. W. Kim, B. S. Choi, Y. S. Chang, and C. W. Park, 2014. Fenofibrate improves renal lipotoxicity through activation of AMPK-PGC-1α in db/db mice. *PLoS ONE* 9.

26. Kim, M. Y., J. H. Lim, H. H. Youn, Y. A. Hong, K. S. Yang, H. S. Park, S. Chung, S. H. Koh, S. J. Shin, B. S. Choi, H. W. Kim, Y. S. Kim, J. H. Lee, Y. S. Chang, and C. W. Park, 2013. Resveratrol prevents renal lipotoxicity and inhibits mesangial cell glucotoxicity in a manner dependent on the AMPK-SIRT1-PGC1α axis in db/db mice. *Diabetologia* 56:204–217.

27. Kim, Y., J. H. Lim, M. Y. Kim, and E. N. Kim, 2018. The Adiponectin Receptor Agonist AdipoRon Ameliorates Diabetic Nephropathy in a Model of Type 2 Diabetes. *Journal of American Society of Nephrology* 29:1108–1127.

28. Park, H. S., J. H. Lim, M. Y. Kim, Y. Kim, Y. A. Hong, S. R. Choi, S. Chung, H. W. Kim, B. S. Choi, Y. S. Kim, Y. S. Chang, and C. W. Park, 2016. Resveratrol increases AdipoR1 and AdipoR2 expression in type 2 diabetic nephropathy. *Journal of Translational Medicine* 14:1–13.

29. Hwang, S. D., J. H. Song, Y. Kim, J. H. Lim, M. Y. Kim, E. N. Kim, Y. A. Hong, S. Chung, B. S. Choi, Y. S. Kim, and C. W. Park, 2019. Inhibition of lymphatic proliferation by the selective VEGFR-3 inhibitor SAR131675 ameliorates diabetic nephropathy in db/db mice. *Cell Death and Disease* 10:1–16.

30. Johnson, R. J., J. Fboege, A. Yoshimura, H. Lida, W. G. Couser, C. E. Alpers pJ Johnson, J. Floege, A. Yoshimura, H. Lida, W. Couser, and C. Alpers, 1992. The Activated Mesangial Cell: A Glomerular "Myofibroblast"? *Journal of the American Society of Nephrology* 190:S190–S197.

31. Thomas, H. Y., and A. N. Ford Versypt, 2022. Pathophysiology of mesangial expansion in diabetic nephropathy: mesangial structure, glomerular biomechanics, and biochemical signaling and regulation. *Journal of Biological Engineering* 16.

32. Liu, Y., 2006. Renal fibrosis: New insights into the pathogenesis and therapeutics. *Kidney International* 69:213–217.

33. Simonson, M., 2007. Phenotypic transitions and fibrosis in diabetic nephropathy. *Kidney International* 71:846–854.

34. Li, H., P. Rong, X. Ma, W. Nie, Y. Chen, J. Zhang, Q. Dong, M. Yang, and W. Wang, 2020. Mouse Umbilical Cord Mesenchymal Stem Cell Paracrine Alleviates Renal Fibrosis in Diabetic Nephropathy by Reducing Myofibroblast Transdifferentiation and Cell Proliferation and Upregulating MMPs in Mesangial Cells. *Journal of Diabetes Research* 2020.

35. Oh, J. H., H. Ha, M. R. Yu, and H. B. Lee, 1998. Sequential effects of high glucose on mesangial cell transforming growth factor-β1 and fibronectin synthesis. *Kidney International* 54:1872–1878.

36. Hong, S. W., M. Isono, S. Chen, M. C. Iglesias-De La Cruz, D. C. Han, and F. N. Ziyadeh, 2001. Increased glomerular and tubular expression of transforming growth factor-β1, its type II receptor, and activation of the smad signaling pathway in the db/db mouse. *American Journal of Pathology* 158:1653–1663.

37. Chen, S., M. C. Iglesias-de la Cruz, B. Jim, S. W. Hong, M. Isono, and F. N. Ziyadeh, 2003. Reversibility of established diabetic glomerulopathy by anti-TGF-β antibodies in db/db mice. *Biochemical and Biophysical Research Communications* 300:16–22.

38. Sáez, P., E. Peña, M. Ángel Martínez, and E. Kuhl, 2013. Mathematical modeling of collagen turnover in biological tissue. *Journal of Mathematical Biology* 67:1765–1793.

39. Rikard, S. M., T. L. Athey, A. R. Nelson, S. L. Christiansen, J. J. Lee, J. W. Holmes, S. M. Peirce, and J. J. Saucerman, 2019. Multiscale Coupling of an Agent-Based Model of Tissue Fibrosis and a Logic-Based Model of Intracellular Signaling. *Frontiers in Physiology* 10.

40. Sutariya, B., D. Jhonsa, and M. N. Saraf, 2016. TGF-β: The connecting link between nephropathy and fibrosis. *Immunopharmacology and Immunotoxicology* 38:39–49.

41. Saito, D., Y. Maeshima, T. Nasu, H. Yamasaki, K. Abe, H. Sugiyama, H. Sonoda, Y. Sato, and H. Makino, 2011. Amelioration of renal alterations in obese type 2 diabetic mice by vasohibin-1, a negative feedback regulator of angiogenesis. *American Journal of Physiology - Renal Physiology* 300:873–886.

42. Terami, N., D. Ogawa, H. Tachibana, T. Hatanaka, J. Wada, A. Nakatsuka, J. Eguchi, C. Sato Horiguchi, N. Nishii, H. Yamada, K. Takei, and H. Makino, 2014. Long-term treatment with the sodium glucose cotransporter 2 inhibitor, dapagliflozin, ameliorates glucose homeostasis and diabetic nephropathy in db/db mice. *PLoS ONE* 9:1–13.

43. Min, D., J. G. Lyons, J. Bonner, S. M. Twigg, D. K. Yue, and S. V. McLennan, 2009. Mesangial cell-derived factors alter monocyte activation and function through inflammatory pathways: Possible pathogenic role in diabetic nephropathy. *American Journal of Physiology - Renal Physiology* 297:1229–1237.

44. Yamagishi, S. I., Y. Inagaki, T. Okamoto, S. Amano, K. Koga, M. Takeuchi, and Z. Makita, 2002. Advanced glycation end product-induced apoptosis and overexpression of vascular endothelial growth factor and monocyte chemoattractant protein-1 in human-cultured mesangial cells. *Journal of Biological Chemistry* 277:20309–20315.

45. Sun, M., Y. Li, W. Bu, J. Zhao, J. Zhu, L. Gu, P. Zhang, and Z. Fang, 2017. DJC Suppresses Advanced Glycation End Products-Induced JAK-STAT Signaling and ROS in Mesangial Cells. *Evidence-based Complementary and Alternative Medicine* 2017:5–7.

46. Iacobini, C., S. Menini, C. Blasetti Fantauzzi, C. M. Pesce, A. Giaccari, E. Salomone, A. Lapolla, M. Orioli, G. Aldini, and G. Pugliese, 2018. FL-926-16, a novel bioavailable carnosinase-resistant carnosine derivative, prevents onset and stops progression of diabetic nephropathy in db/db mice. *British Journal of Pharmacology* 175:53–66.

47. Sohn, E., J. Kim, C. S. Kim, Y. M. Lee, K. Jo, S. D. Shin, J. H. Kim, and J. S. Kim, 2013. The extract of litsea japonica reduced the development of diabetic nephropathy via the inhibition of advanced glycation end products accumulation in db/db mice. *Evidence-based Complementary and Alternative Medicine* 2013.

48. Do, M. H., J. Hur, J. Choi, Y. Kim, H. Y. Park, and S. K. Ha, 2018. Spatholobus suberectus ameliorates diabetes-induced renal damage by suppressing advanced glycation end products in db/db mice. *International Journal of Molecular Sciences* 19.

49. Hao, W., C. Marsh, and A. Friedman, 2015. A mathematical model of idiopathic pulmonary fibrosis. *PLoS One* 10:e0135097.

50. Rabbani, N., and P. J. Thornalley, 2018. Glycation- and/or Polyol Pathway-Inducing Complications. *In* Encyclopedia of Endocrine Diseases, 170–179.

51. Menini, S., C. Iacobini, L. de Latouliere, I. Manni, V. Ionta, C. Blasetti Fantauzzi, C. Pesce, P. Cappello, F. Novelli, G. Piaggio, and G. Pugliese, 2018. The advanced glycation end-product Nϵ-carboxymethyllysine promotes progression of pancreatic cancer: implications for diabetes-associated risk and its prevention. *Journal of Pathology* 245:197–208.

52. Doan, V. M., C. Chen, X. Lin, V. P. Nguyen, Z. Nong, W. Li, Q. Chen, J. Ming, Q. Xie, and R. Huang, 2015. Yulangsan polysaccharide improves redox homeostasis and immune impairment in D-galactose-induced mimetic aging. *Food and Function* 6:1712–1718.

53. Brings, S., T. Fleming, M. Freichel, M. U. Muckenthaler, S. Herzig, and P. P. Nawroth, 2017. Dicarbonyls and advanced glycation end-products in the development of diabetic complications and targets for intervention. *International Journal of Molecular Sciences* 18.

54. Yuan, Y., H. Sun, and Z. Sun, 2017. Advanced glycation end products (AGEs) increase renal lipid accumulation: A pathogenic factor of diabetic nephropathy (DN). *Lipids in Health and Disease* 16:1–9.

55. Pugliese, G., F. Pricci, C. Pesce, G. Romeo, E. Lenti, V. Caltabiano, M. Vetri, F. Purrello, and U. Di Mario, 1997. Early, but Not Advanced, Glomerulopathy Is Reversed by Pancreatic Islet Transplants in Experimental Diabetic Rats. *Diabetes* 46:1198–1206.

56. Mauer, S., D. Sutherland, M. Steffes, R. Leonard, J. Najarian, A. Michael, and D. Brown, 1974. Pancreatic islet transplantation: Effects on the glomerular lesions of experimental diabetes in the rat. *Diabetes* 23:748–753.

57. Mauer, S. M., M. W. Steffes, D. E. Sutherland, Najarian-S, A. F. Michael, and D. M. Brown, 1975. Studies of the rate of regression of the glomerular lesions in diabetic rats treated with pancreatic islet transplantation. *Diabetes* 24:280–285.

58. Lee, C. S., S. M. Mauer, D. M. Brown, D. E. Sutherland, A. F. Michael, and J. S. Najarian, 1974. Renal transplantation in diabetes mellitus in rats. *The Journal of experimental medicine* 139:793–800.

59. Steffes, M. W., D. M. Brown, J. M. Basgen, and S. M. Mauer, 1980. Amelioration of mesangial volume and surface alterations following islet transplantation in diabetic rats. *Diabetes* 29:509–515.

60. Kelly, D. J., R. E. Gilbert, A. J. Cox, T. Soulis, G. Jerums, and M. E. Cooper, 2001. Aminoguanidine ameliorates overexpression of prosclerotic growth factors and collagen deposition in experimental diabetic nephropathy. *Journal of the American Society of Nephrology* 12:2098–2107.

61. Forbes, J. M., V. Thallas, M. C. Thomas, H. W. Founds, W. C. Burns, G. Jerums, and M. E. Cooper, 2003. The breakdown of pre-existing advanced glycation end products is associated with reduced renal fibrosis in experimental diabetes. *The FASEB Journal* 17:1762–1764.

62. Lassila, M., K. K. Seah, T. J. Allen, V. Thallas, M. C. Thomas, R. Candido, W. C. Burns, J. M. Forbes, A. C. Calkin, M. E. Cooper, and K. A. Jandeleit-Dahm, 2004. Accelerated nephropathy in diabetic apolipoprotein E-knockout mouse: Role of advanced glycation end products. *Journal of the American Society of Nephrology* 15:2125–2138.

Table 1: Parameter values, units and source for glomerular fibrosis model.

Parameter	Symbol	Value	Units	Source
AGE degradation rate	d_{AGE}	$8.7E-3$	day^{-1}	Rabbani2018 and estimated
AGE baseline conc'n	AGEss	$1.50E-07$	g/ml	Yuan2017 and Menini2018
Production rate of AGE	λ_{AGE}	$6.58E+08$	$(g/ml)^{-5}day^{-1}$	Estimated
Power term for glucose conc'n	m	6	Unitless	Estimated
MCP dynamics				
Baseline MCP production	Po	$9.25E-11$	$(g/ml)day^{-1}$	Estimated
MCP degradation rate	d_P	1.73	day^{-1}	(13)
Baseline MCP concentration in vitro	Pss	$1.60E-10$	g/ml	(44)
Production rate of MCP by MC	λ_{Pmc}	$2.74E-10$	day^{-1}	Estimated
AGE saturation constant for MCP production	K_{AGE}	$1.14E-06$	g/ml	Estimated
Macrophage dynamics				
Power term for macrophage population	n	4.00	Unitless	Estimated
Recruitment rate for macrophages	alpha	$7.89E+09$	day^{-1}	Estimated
Macrophage death/removal rate	d_M	52.00	day^{-1}	Estimated
MCP saturation constant for macrophage recruitment	K_P	$5.00E-09$	g/ml	(13)
Monocyte concentration	Mo	$5.00E-05$	g/ml	(13)
TGF-β dynamics				
Baseline production of TGF-β	T_{Bknot}	$3.22E-07$	$(g/ml)day^{-1}$	Estimated
Production rate of T_B by macrophages	λ_{TBM}	$7.5*10^-6$	day^{-1}	Estimated
Degradation rate of T_B	d_{TB}	$3.33E+02$	g/ml	(13)
Activated mesangial cell dynamics				
Baseline α-sma production	mao	$5.64E-04$	$(g/ml)day^{-1}$	Estimated
α-sma production rate	λ_{maT}	$4E-3$	day^{-1}	Estimated
TGF-β saturation constant for activation of mc	K_{TB}	$2.5E-09$	g/ml	Estimated
Activated mesangial cell death	$d_{ma-vitro}$	0.0166	day^{-1}	(13)
Power term for mesangial cell activation	n1	3.5	unitless	Estimated
Activated mesangial cell death	$d_{ma-vivo}$	$5E+1$	day^{-1}	Estimated
MMP, TIMP and collagen dynamics				
Production rate of MMP by macrophages	λ_{QM}	$3.00E-08$	day^{-1}	Estimated
Binding rate of MMP to TIMP	d_{QQr}	$4.98E+08$	$(g/ml)^{-1}day^{-1}$	(13)
Degradation rate of MMP	d_Q	4.32	day^{-1}	(13)
Production rate of TIMP by macrophages	$\lambda_{Q}rM$	$6.00E-09$	day^{-1}	Estimated
Binding rate of TIMP to MMP	d_{QrQ}	$1.04E+09$	$(g/ml)^{-1}day^{-1}$	(13)
Degradation rate of TIMP	d_{Qr}	21.60	day^{-1}	(13)
Production rate of collagen by mesangial cells	$\lambda_{\rho m}$	$3.00E-03$	day^{-1}	(13)
Production rate of collagen by ma	$\lambda_{\rho ma}$	10	day^{-1}	Estimated
Degradation rate of collagen	d_{rho}	$3.70E-01$	day^{-1}	(13)
Degradation rate of collagen by MMP	d_{rhoQ}	$5.00E-05$	$(g/ml)^{-1}day^{-1}$	Estimated

Table 2: Estimated initial values for model species

Initial value for Species	Symbol	Value	Units	Source
AGE	AGEss	$1.5E10^-7$	g/ml	Yuan2017 and Menini2018
MCP	MCPss	$1.78E10^-10$	g/ml	Estimated
Macrophages	Mss	$1.04E10^-2$	g/ml	Estimated
TGF-β	TGF-βss	$1.2E10^-9$	g/ml	Estimated
Activated mesangial cell	mass	$1.5E-3$	g/ml	Estimated
MMP	Qss	$7.22E10^-11$	g/ml	Estimated
TIMP	Qrss	$2.9E10^-12$	g/ml	Estimated
Collagen	ρss	$4.63E-2$	g/ml	Estimated